Angewandte Chemie

Eine Zeitschrift der Gesellschaft Deutscher Chemiker

Supporting Information

69451 Weinheim, Germany

Anomalous Surface Compositions of Stoichiometric Mixed Oxide Compounds**

*Sergiy V. Merzlikin, Nikolay N. Tolkachev, Laura E. Briand, Thomas Strunskus, Christof Wöll, Israel E. Wachs, and Wolfgang Grünert**

anie_201001804_sm_miscellaneous_information.pdf

Experimental

Materials. Preparation and structural characterization of the bulk molybdate and vanadate catalytic materials employed have been described in earlier reports[1-3]. Briefly, the bulk molybdates and vanadates not containing bismuth were made by coprecipitation of $(NH_4)_6Mo_7O_{24}$*4 H_2O and the corresponding metal nitrates or via a citrate-based route from NH_4VO_3 and the nitrates using Alfa Aesar chemicals (99.9 %) (Ref. [1, 2] and references cited therein). The bismuth molybdates phases were made by solid-state reaction between α-Bi_2O_3 and MoO_3 powders (both 99.9 %) at 1110 K in flowing oxygen[3]. Their crystalline structures and absence of residual α-Bi_2O_3 and MoO_3 phases in these materials has been shown by XRD and Raman spectroscopy[1-4]. Model supported vanadate and molybdate catalysts (V_2O_5/ZrO_2, V_2O_5/Al_2O_3, MoO_3/CeO_2) containing surface VOx and MoOx overlayers were prepared by incipient wetness impregnation of the supports (ZrO_2, Degussa, 34 m^2/g; Al_2O_3, Engelhard, 222 m^2/g; CeO_2, SKK, 36 m^2/g) with solutions of vanadium triisopropoxide ($VO(O\text{-}Pr^i)_3$, (Alfa, 95-98% purity) in methanol or with an aqueous solution of ammonium heptamolybdate $(NH_4)_6Mo_7O_{24}$*4 H_2O[5, 6]. Their vanadium (molybdenum) contents are given in Table S1 where they are also related to the theoretical monolayer coverage [5, 6].

In our study, the surfaces of all conventionally prepared bismuth molybdate phases were found to be contaminated by potassium (bulk K content not quantified in the present surface investigation). Similar contaminations were found in $BiVO_4$ prepared from different precursors and in many commercially available Bi chemicals[7]. For this reason, some bismuth molybdate phases were purified by methods that involve zone refining. For instance, prefabricated α-$Bi_2MoO_3O_{12}$ was purified by rf skull melting where the material

was placed in a water-chilled copper crucible equipped with heat-exchange fingers and was melted by rf from a surrounding coil. After locally initiating the melt by a small graphite disc rf receptor, further melting occurred by resistive heating in the ion-conducting melt. While the crucible was lowered out of the coil, decoupling, congruent solidification, and crystallization occurred from the bottom upward.

The remaining phases were prepared by solid-state reaction in covered Coors alumina (99.9 %) crucibles at temperatures slightly below the peritectic temperatures of the respective phases. Crystals were grown by melting prereacted powders in an alumina boat in a horizontal furnace; the composition was chosen to be close to the point where the peritectic line joins the liquidus line so that crystals of the desired phase form upon cooling with a small temperature gradient. Only the first crystals were recovered as they should be of superior purity.

Table S1 – Supported catalysts investigated in this study

Catalyst	wt-% V_2O_5 (MoO_3)[a]	BET surface area, m^2/g	V (Mo) atoms /nm^2	% of theoretical monolayer[b]
V_2O_5/ZrO_2	4.0	35	7.5	95
V_2O_5/Al_2O_3	15.3	170	6.0	75
MoO_3/CeO_2	2.7	31	3.6	78

[a]by ICP-OES

[b]theoretical monolayer coverage ≈ 8 V atoms/nm^2 for the V-Zr-O and V-Al-O systems, and ≈ 4.6 Mo atoms/nm^2 for the Mo-Ce-O system.

Spectroscopic measurements. Laboratory X-ray photoelectron and ion scattering spectra were measured with a Leybold surface analysis system equipped with X-ray and ion

sources and an EA 10/100 electron (ion) analyzer with multi-channel detection (Specs). The samples were calcined in flowing synthetic air (20 % O_2/N_2) at 730 K for 1 h before introducing them into the spectrometer vacuum without further contact with the ambient atmosphere. XPS was measured using Al Kα or Mg Kα excitation (1486.6 or 1253.6 eV). Averaged "surface" atomic ratios (cf. Table 1) were evaluated from the intensity ratios between the main elemental lines using a traditional procedure (ionization cross sections[8] together with an empirical response function relating spectrometer sensitivity to the photoelectron kinetic energy). Only excitation lines with binding energies below 100 eV (V 3p, Zr 4p, Mo 4p, Fe 3p) were employed for depth profile analysis in order to avoid complications due to different escape depths and analyzer sensitivities (*vide infra*).

LEIS spectra were measured with 1000 eV or 2000 eV He^+ ions (E_0 given in the legends) taking many spectra in series to observe the trends of elemental intensity during erosion of the surface layers. For intensity evaluation, incompletely separated signals were fitted on linear backgrounds if not stated otherwise.

Synchrotron XPS was measured at the HESGM beamline of the Berlin electron storage ring BESSY-II. With entry and exit slits set to 200 µm, an energy resolution of ≈ 0.4 eV at 300 eV excitation energy was achieved, with a spot size of 1.2 mm x 0.5 mm at normal incidence to the sample. The analysis chamber (base pressure < $2*10^{-10}$ mbar) was equipped with standard facilities for sample preparation, a VG Microtech CLAM2 energy analyzer, and a VG Microtech twin anode X-ray source (XR3E2), which was operated at 12 kV and 24 mA. Surface charging is a severe problem in synchrotron XPS with oxide materials, which has impeded similar measurements with a number of materials used in this study. The samples were calcined as described above, mounted on the sample holder

in flowing argon, inserted into the sample lock and pumped down on the roughing stage rapidly, with air contact confined to less than 30 seconds. The binding energy (BE) scale was corrected relative to O 2s = 21.0 eV, which was obtained with the laboratory sources and a C 1s reference (284.5 eV).

Depth profile modeling. The extraction of approximate concentration depth profiles from XPS intensity ratios is described in detail in ref. [9] where the method has been referred to as excitation-energy resolved XPS (ERXPS). Experimental intensity ratios $P_k = I_{A,k} / I_{B,k}$, measured for different escape depths $\lambda_{k,}$ were modeled as averages of contributions from different depths z:

$$P_{k,calc} = \frac{I_{A,k}}{I_{B,k}} = \frac{\sigma_A(h\nu_k)\, S(E_{kin,A}) \int_0^\infty \rho_A(z) \exp\left(-z/\lambda_{A,k}\right) dz}{\sigma_B(h\nu_k) S(E_{kin,B}) \int_0^\infty \rho_B(z) \exp\left(-z/\lambda_{B,k}\right) dz} \qquad (1)$$

In which $S(E_{kin,\,i})$ are analyzer sensitivities that are cancelled in our approach because only lines of similar binding energy are included *(vide supra*). Correlations of mean free path λ_i and ionization cross section σ_t with the kinetic energy E_{kin} were taken from the literature[8, 10]. The depth concentration profiles $\rho_A(z)$ and $\rho_B(z)$ (in atoms nm^{-3}), which are interrelated by stoichiometry, were represented by assumed functions, e.g. exponential, linear, stepwise, Gaussian, etc., and the parameters of these functions were estimated by fitting the model $P_{k,calc}$ (according to (1)) against the measured intensity ratios $P_k = f(\lambda_{i,k})$ using the software package "Depth profiling" (© N. N. Tolkachev). The method was validated with self-assembled monolayers of octadecanethiol on gold samples of different roughness, where a somewhat more involved algorithm was required due to the large density differences between components (Au, organic layer)[9].

Table S2 – Conventional XPS analysis of additional bismuth molybdate phases [a]

Oxide	Stoichiometry Mo/Bi)	"Surface" Mo/Bi[b]
α-$Bi_2Mo_2O_9$(K)	1	1.41 (K : Bi = 0.10)
$Bi_6Mo_2O_{15}$(K)	0.33	0.24 (K : Bi = 0.07)
$Bi_{38}Mo_7O_{78}$(K)	0.18	0.19 (K : Bi = 0.22)
γ(L)-Bi_2MoO_6	0.5	0.43

[a]no bulk MoO_3 detected in Raman analysis

[b]photoionization cross sections of Ref. [10] used together with an empirical function for kinetic-energy dependence of spectrometer sensitivity.

Literature

1. L. E. Briand, A. H. Hirt, I. E. Wachs, *J. Catal.* 202, 268 (2001).
2. L. E. Briand, J.-M. Jehng, L. Cornaglia, A. H. Hirt, I. E. Wachs, *Catal. Today* 78, 257 (2003).
3. D. J. Buttrey, D. A. Jefferson, J. M. Thomas, *Phil. Mag. A* 53, 897 (1986).
4. F. D. Hardcastle, I. E. Wachs, *J. Phys. Chem.* 95, 10763 (1991).
5. L. E. Briand, O. P. Tkachenko, G. M., I. E. Wachs, W. Grünert, *Surf. Interface Anal.* 36, 238 (2004).
6. L. E. Briand, O. P. Tkachenko, M. Guraya, X. Gao, I. E. Wachs, W. Grünert, *J. Phys. Chem. B* 108, 4823 (2004).
7. S. Merzlikin, W. Grünert, I. E. Wachs, unpublished results.
8. J. J. Yeh, I. Lindau, *At. Data Nucl. Data* 32, 2 (1985).
9. S. V. Merzlikin, N. N. Tolkachev, T. Strunskus, G. Witte, T. Glogowski, C. Wöll, W. Grünert, *Surf. Sci.* 602, 755 (2008).
10. S. Tanuma, C. J. Powell, D. R. Penn, *Surf. Interface Anal.* 21, 165 (1994).

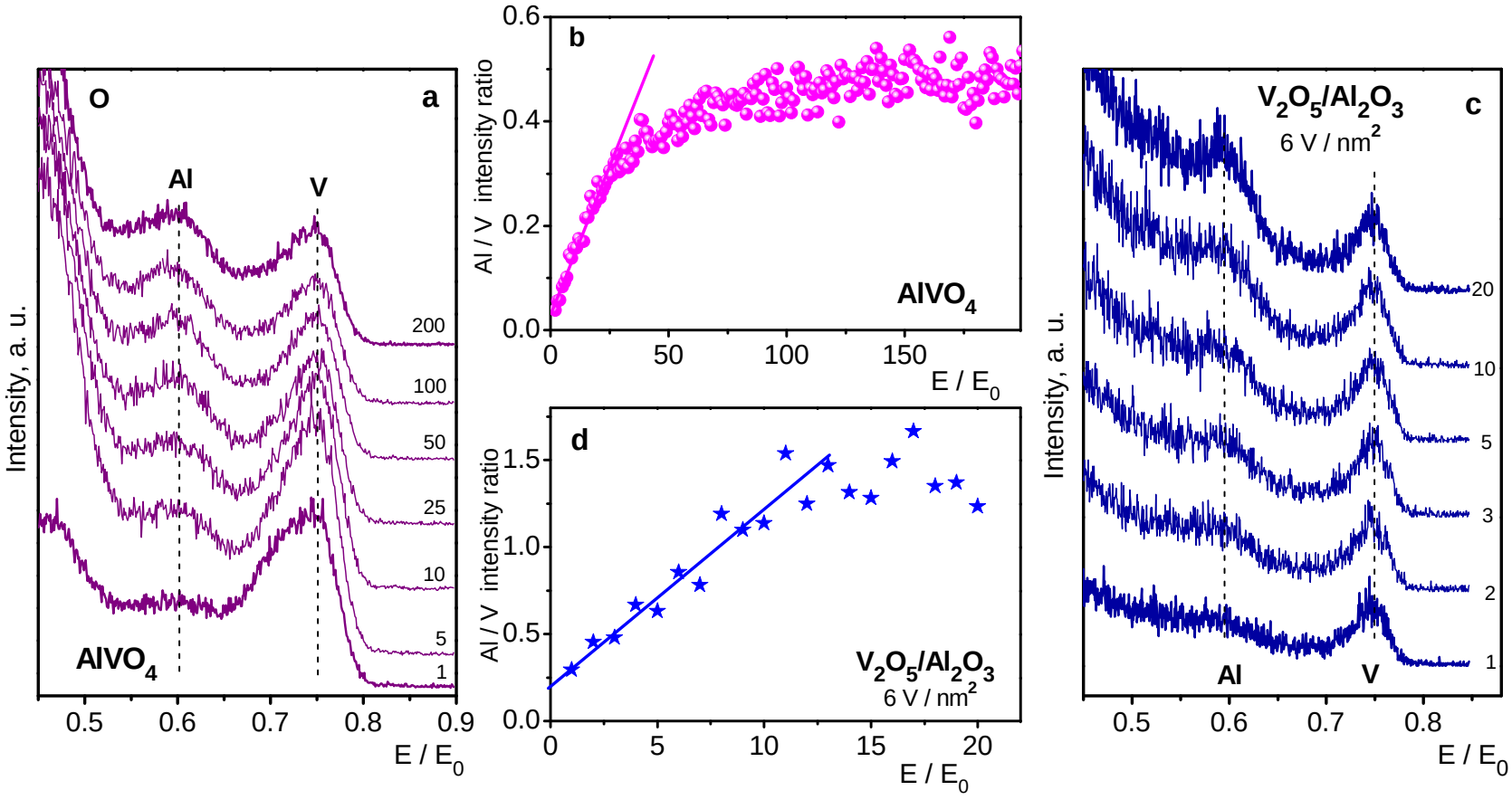

Fig. S1. LEIS sputter series and intensity trends measured with V-Al-O mixed oxides. a and b – $AlVO_4$, E_0 = 1000 eV, c and d – 15.3 wt-% V_2O_5/Al_2O_3 (V content - ca. 75 % of the theoretical monolayer coverage, cf. Table S1), E_0 = 1000 eV.

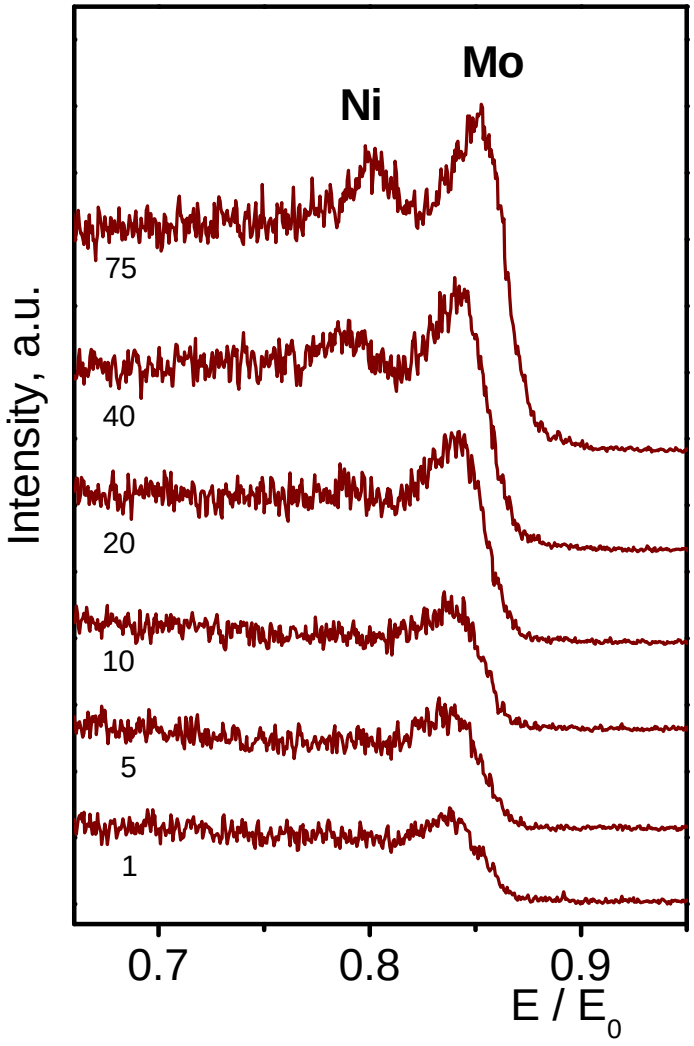

Fig. S2 LEIS sputter series of bulk $NiMoO_4$. E_0 = 2000 eV.

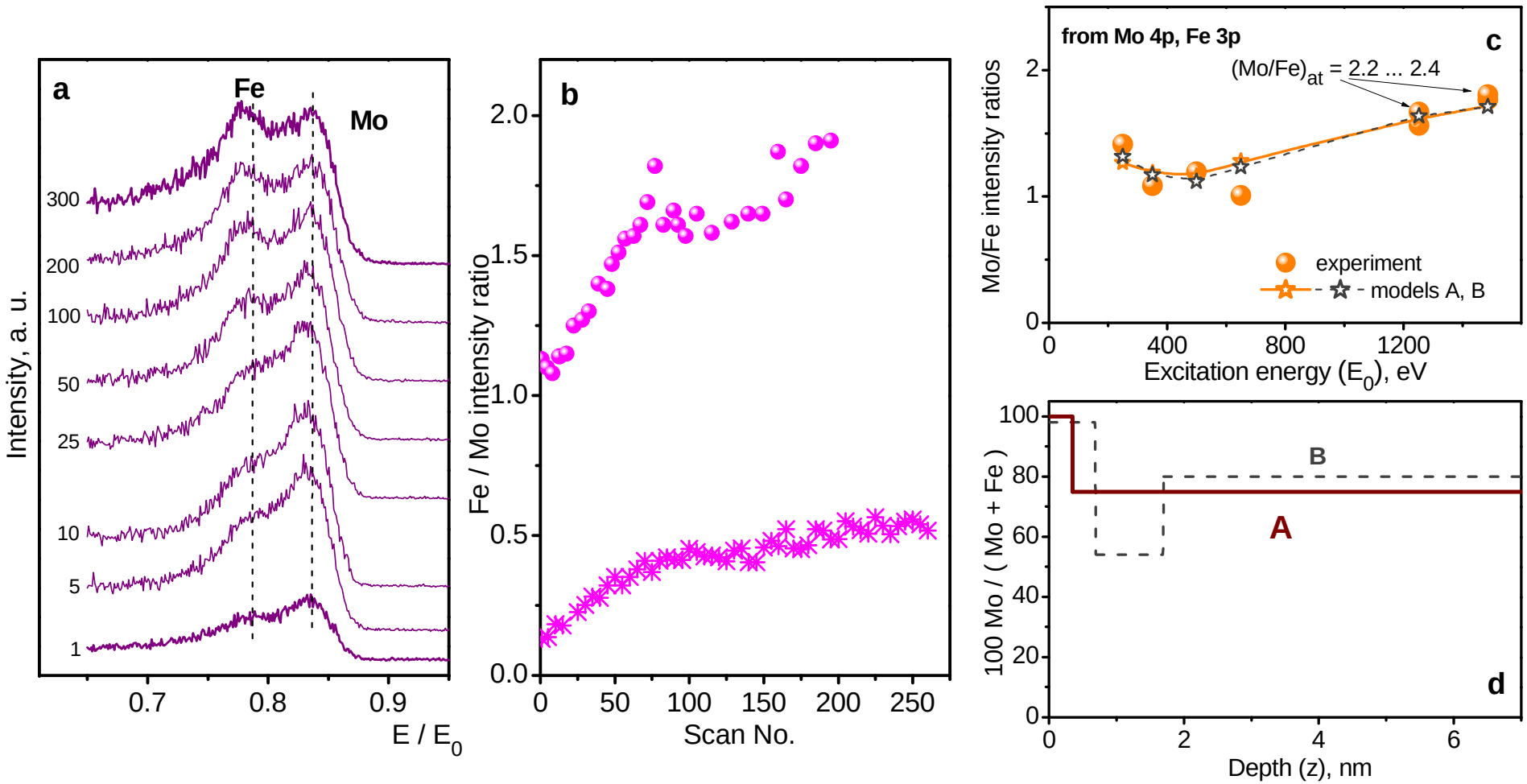

Figure S3. Analysis of the surface region of $Fe_2(MoO_4)_3$ by LEIS and ERXPS. a and b – LEIS sputter series (E_0 = 1000 eV) and intensity trends, with different treatment of the baseline, c) comparison of measured XPS intensity ratios with data calculated from the best available Mo depth distribution (see d), d – best model for depth distribution of Mo percentage. Note that Fig. S3c shows intensity ratios, not atomic ratios. The modeled Mo percentage (Fig. S3 d) does not decay to the theoretical value of 60 % (corresponding to Mo/Fe = 1.5). This agrees with the analysis via the Mo 4p/ Fe 3p lines (see comment in Fig. S3c) and the results of conventional XPS (Table 1 – Mo/Fe = 1.83) Obviously, the whole XPS sampling region of $Fe_2(MoO_4)_3$ is enriched in Mo oxide species, but the external surface layer is Mo-enriched beyond this, hardly exposing any iron.

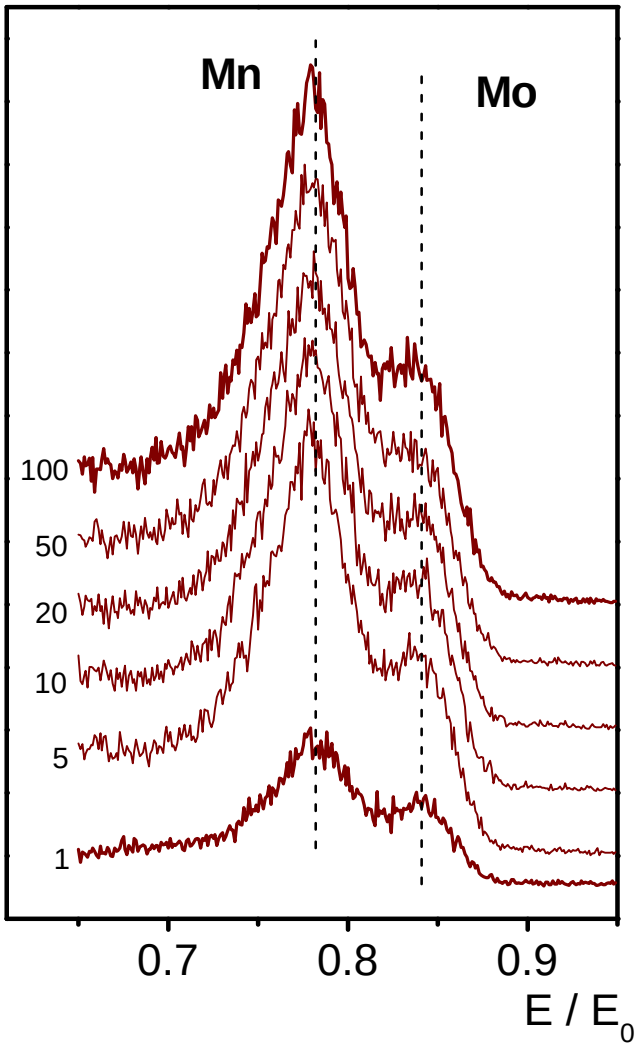

Figure S4. LEIS sputter series of bulk $MnMoO_4$. E_0 = 1000 eV.

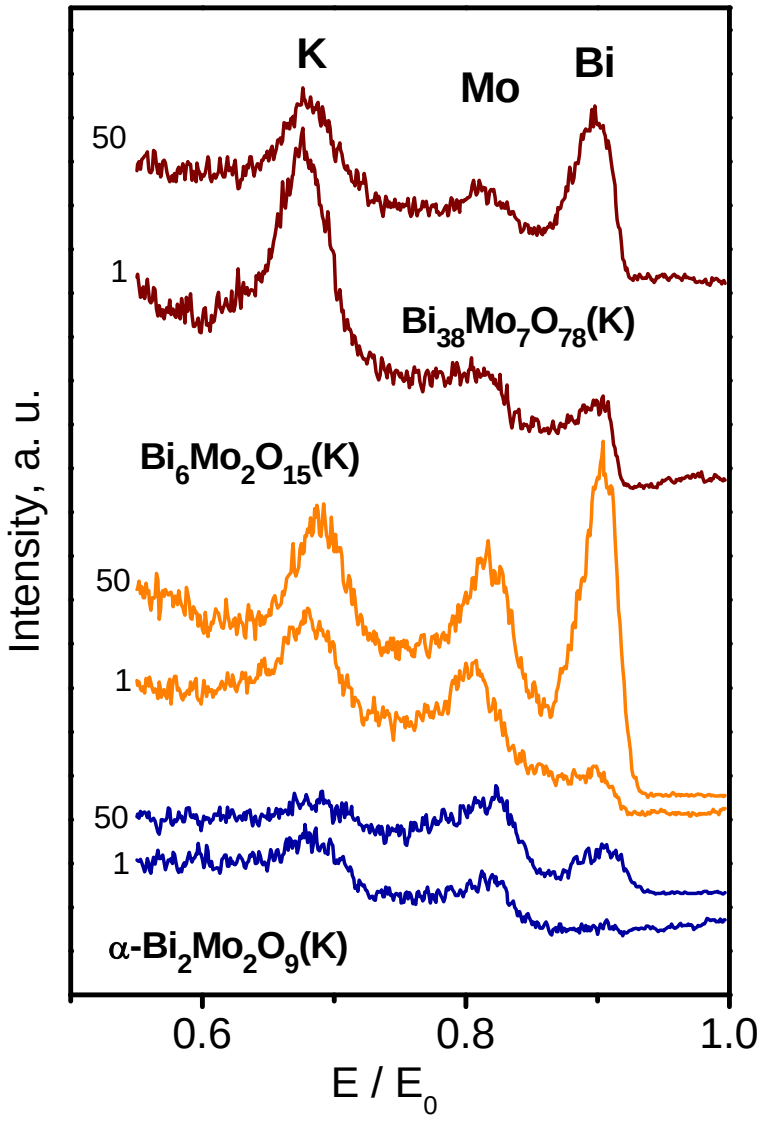

Fig. S5. LEIS sputter series (1st and 50th scan) of potassium-contaminated bulk bismuth molybdate phases: $Bi_{38}Mo_7O_{78}$(K), $Bi_6Mo_2O_{15}$(K), and α-$Bi_2Mo_2O_9$(K), E_0 = 1000 eV.

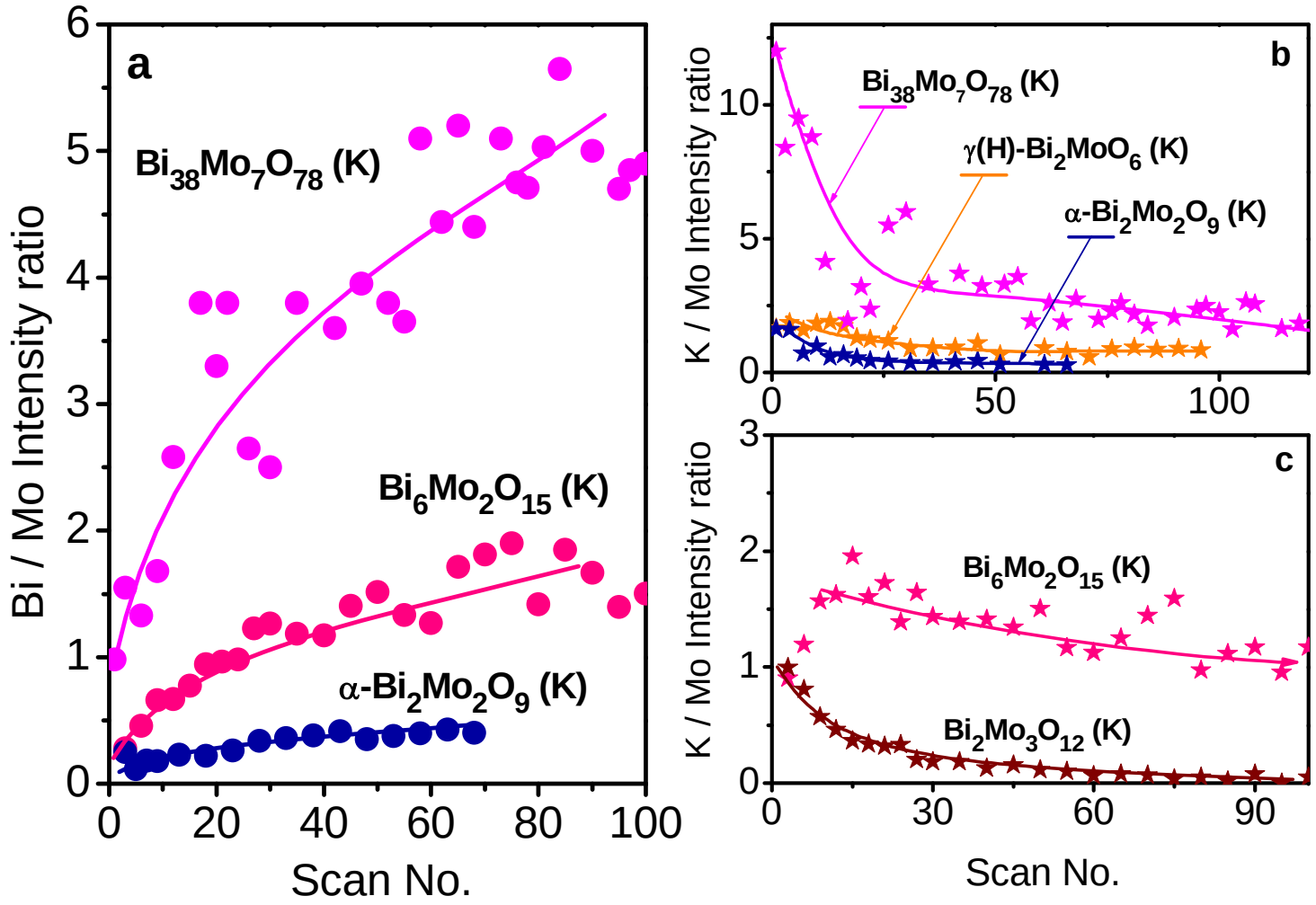

Fig. S6. Intensity trends from LEIS sputter series with K-doped bismuth molybdate phases (cf. Fig. S4 and Fig. 5). a – Bi/Mo intensity trends, b, c - K/Mo intensity trends of samples shown in Fig. S5 and in Fig. 6.

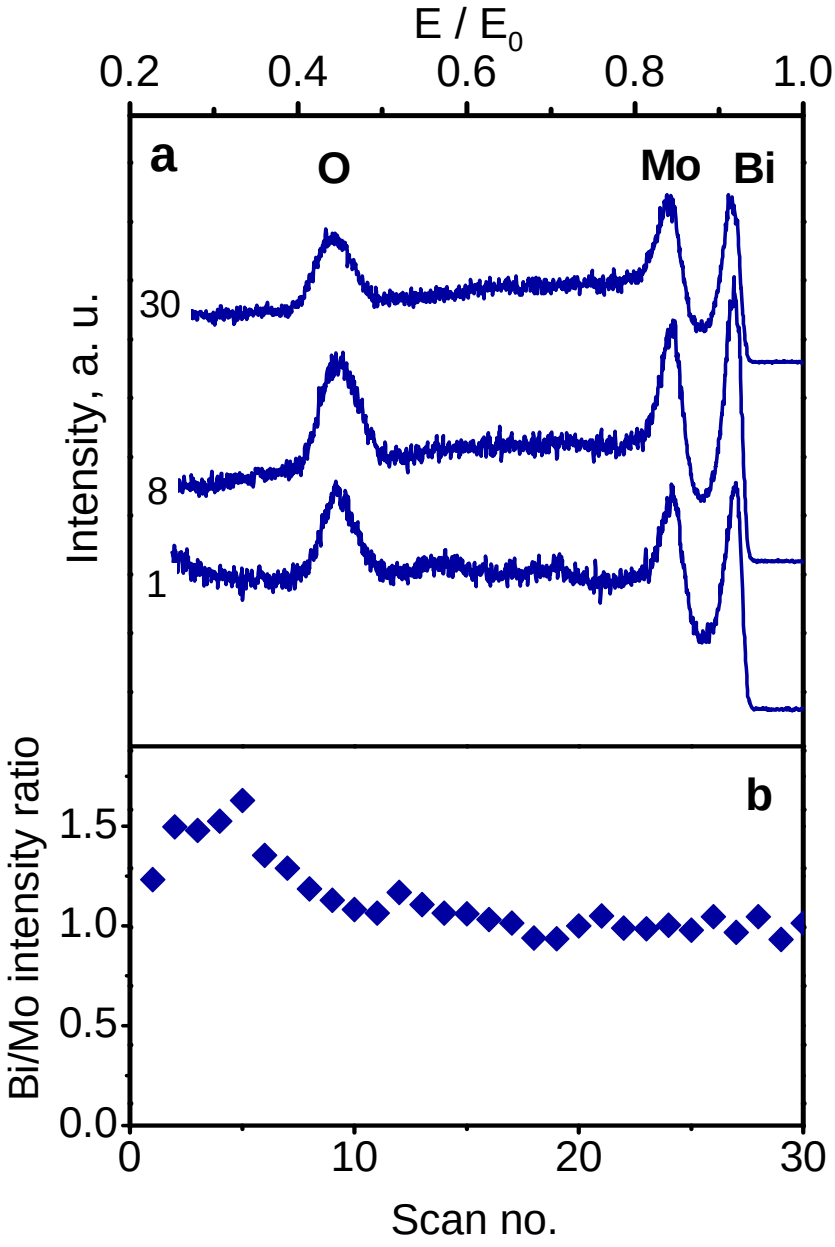

Fig. S7. LEIS sputter series and Bi/Mo intensity trend measured with pure γ(L)-Bi_2MoO_6